The following publication Dou, J., Xu, B., & Dou, L. (2020). Impact Assessment of the Asynchronous Clocks Between Reference and User Receivers in Differential Pseudolite Navigation System. IEEE Sensors Journal, 21(1), 403-411 is available at https://doi.org/10.1109/JSEN.2020.3014103

Impact assessment of the asynchronous clocks between reference and user receivers in differential pseudolite navigation system

Jie Dou, Bing Xu, and Lei Dou

***Abstract*—Compared with the Global Navigation Satellite System (GNSS), the asynchronous pseudolite (PL) navigation system does not provide corrections for the frequency deviation between PL signals. To realize precise positioning, a reference receiver is utilized to reduce the effect of frequency deviation between PLs via the differential method using carrier phase measurements. However, there exists time deviation between the user and reference receivers due to their asynchronous clocks. With this time deviation, the effect of frequency deviation between PLs cannot be removed thoroughly. Theoretical derivation and experimental verification indicate that the residual error in double difference of carrier phase measurements is proportional to the frequency deviation between PLs and the time deviation between receivers. To solve this problem, two approaches, refer to hardware and software methods, are proposed, which are experimentally proven to be feasible.**

***Index Terms*—Global Navigation Satellite System, Pseudolites, clock synchronization, oven controlled crystal oscillators**

I. Introduction

Global navigation satellite system (GNSS) has been widely and successfully used in various kinds of applications [1-2]. However, in GNSS-challenging or GNSS-denied environments, its performance is highly degraded such as highly urbanized areas where multipath interference and non-line-of-sight reception can introduce large positioning errors [3]. Pseudolites (PLs), transmitting GNSS-like signals [4], have been widely used in applications where GNSS signals are severely attenuated or not available, e.g. indoors or very deep urban areas [5-7]. Augmented by PLs, conventional GNSS receivers can achieve better accuracy and availability [7, 8]. An independent positioning system can also be developed when there are four or more PLs available, to realize a 3D-position and time fixes [9-11]. However, there are several fundamental issues that limit the effectiveness of an independent PL positioning system such as near-far problem, multipath effect, and clock synchronization. A number of techniques for addressing these issues have been proposed in the literature [12-16].

In terms of clock synchronization, the PL positioning systems can be classified into two categories, i.e., the synchronous and asynchronous systems. For synchronous PL systems, PLs are strictly time-synchronous [17, 18], potentially allowing single point positioning with the accuracy at centimeter-level using carrier phase measurements. However, stringent synchronization requirements may lead to significant deployment costs. Moreover, biases in measurements could still be present due to multipath or other propagation effects in deep indoor scenarios [19]. For asynchronous PL systems, PLs operate independently. To achieve centimeter-level position, it is essential that all the PLs are accurately time synchronized.

For GNSS satellites, the frequency generation is based on a highly accurate atomic standard, while for PLs, oven controlled crystal oscillators (OCXOs) are typically used as the frequency sources. In general, the generated frequency is offset from the nominal values for both GNSS and PL transmitters. For GNSS and synchronous PL system, corrections for this offset are generated by the ground-based monitoring network periodically and sent to users via navigation messages. However, in an asynchronous PL system, no corrections are available for users, and this frequency offset varies with time due to the poorer frequency stability of OCXOs, compared with atomic clocks. To overcome this problem, Locata utilized a proprietary TimeLoc technology for achieving accurate time synchronization of all PLs [20,21], but it is too expensive for deployments. By sharing a single clock source between PLs, the frequency deviation can be excluded [22]. This is limited by the transmission distance and delay. Daniele et al. [19] and Hyoungmin et al. [23] used a reference receiver to collect the measurements of the PLs signal and generate the frequency correction for each PL, which is referred to the double difference method. Another method for time synchronization is to use the GNSS timing, in which a reference receiver is also needed [24-25]. However, these methods are reasonable only if the reference and user receivers have accurate synchronous clock. Otherwise, there are residual errors. More specifically, with asynchronous clocks, the interval of one epoch is not identical for reference and user receivers. When using carrier phase measurements, the advance in carrier phase during one

This work was supported by National Natural Science Foundation of China (grant number 60904085); Foundation of National Key Laboratory of Transient Physics; and Foundation of Defence Technology Innovation Special Filed.

J. Dou, and L, Dou are with School of National Key Laboratory of Transient Physics, Nanjing University of Science and Technology, Nanjing 210094, China (e-mail: doujienjust@163.com; douleijs@163.com).

B. Xu is with the Interdisciplinary Division of Aeronautical and Aviation Engineering, The Hong Kong Polytechnic University, Kowloon, Hong Kong, China (e-mail: pbing.xu@polyu.edu.hk).

epoch interval is calculated by integrating the carrier Doppler frequency over the interval of one epoch. The Doppler frequency measured by the receiver includes both the motion-induced and the oscillator-induced frequency deviation. Thus, the carrier phase advance due to the frequency deviation of PL signals during one epoch interval is not identical for the reference and user and therefore, it cannot be eliminated thoroughly. The residual would then affect the carrier phase measurement and consequently affect the positioning results. For this reason, we investigated the effect of clock asynchronization of user and reference receivers, and the frequency deviation between PL signals, which is conducted using a self-designed PL navigation system. The contributions of this paper could be summarized as:

(1) Theoretical derivation and a series of experimental verifications were carried out for evaluating the impact of clock asynchronization of user and reference receiver in PL system.

(2) Two approaches, refer to hardware and software methods, are proposed to eliminate the time deviation in PL navigation system, which are experimentally proven to be feasible.

The remainder of this paper is organized as follows: Section II derives the carrier phase double differences positioning algorithm for an asynchronous PL system. Section III reveals the reason why the clock asynchronization affects the carrier phase measurements and the positioning results. To verify this, a series of experiments are conducted in Section IV. At last, conclusions are drawn in Section V.

II. Carrier Phase Double Differences Positioning Algorithm for an Asynchronous PL System

The schematic diagram of an asynchronous PL system is shown in Figure 1. A reference receiver sends its carrier phase measurements to the user receiver via a wireless data link. The carrier phase measurements are modeled as follows:

User:

$$\phi_u^i = \frac{1}{\lambda}\left(R_u^i + c\left(\delta t_u - \delta t^i\right)\right) + N_u^i + \varepsilon_u^i \tag{1}$$

$$\phi_u^j = \frac{1}{\lambda}\left(R_u^j + c\left(\delta t_u - \delta t^j\right)\right) + N_u^j + \varepsilon_u^j \tag{2}$$

Reference:

$$\phi_r^i = \frac{1}{\lambda}\left(R_r^i + c\left(\delta t_r - \delta t^i\right)\right) + N_r^i + \varepsilon_r^i \tag{3}$$

$$\phi_r^j = \frac{1}{\lambda}\left(R_r^j + c\left(\delta t_r - \delta t^j\right)\right) + N_r^j + \varepsilon_r^j \tag{4}$$

where:

ϕ_u^i , ϕ_u^j , ϕ_r^i , ϕ_r^j : user and reference carrier phase measurements of *i*th and *j*th PL in cycles

λ : wavelength of PL carrier

c : the speed of light

R_u^i , R_u^j , R_r^i , R_r^j : geometrical ranges between receivers and PLs

δt_u , δt_r : receiver clock errors

δt^i , δt^j : PL clock errors

N_u^i , N_u^j , N_r^i , N_r^j : ambiguity integers

ε_u^i , ε_u^j , ε_r^i , ε_r^j : residual unmodelled errors

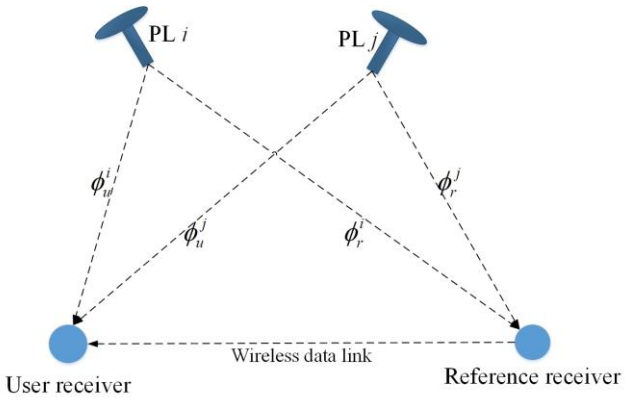

Fig. 1. Schematic diagram of an asynchronous PL system

The single difference is created by differencing carrier phase measurements (user to the *i*-th PL and reference to the *j*-th PL):

$$\begin{aligned} {}^u\nabla^r\phi^i &= \phi_u^i(t) - \phi_r^i(t) \\ &= \frac{1}{\lambda}\left(\left(R_u^i - R_r^i\right) + c\left(\delta t_u - \delta t_r\right)\right) + N_u^i - N_r^i + \varepsilon_u^i - \varepsilon_r^i \end{aligned} \tag{5}$$

$$\begin{aligned} {}^u\nabla^r\phi^j &= \phi_u^j(t) - \phi_r^j(t) \\ &= \frac{1}{\lambda}\left(\left(R_u^j - R_r^j\right) + c\left(\delta t_u - \delta t_r\right)\right) + N_u^j - N_r^j + \varepsilon_u^j - \varepsilon_r^j \end{aligned} \tag{6}$$

A double difference is formed based on the above two single differences:

$$\begin{aligned} {}^i\nabla^j{}_u\Delta_r\phi &= {}^u\nabla^r\phi^i - {}^u\nabla^r\phi^j \\ &= \frac{1}{\lambda}\left(\left(R_u^i - R_r^i\right) - \left(R_u^j - R_r^j\right)\right) + \left(N_u^i - N_r^i\right) - \left(N_u^j - N_r^j\right) \\ &\quad + \left(\varepsilon_u^i - \varepsilon_r^i\right) - \left(\varepsilon_u^j - \varepsilon_r^j\right) \end{aligned} \tag{7}$$

With the formation of the double difference, both the PL and receiver clock-bias terms are removed. The remaining unknowns are the coordinates of the user receiver and the ambiguity integers. Various methods have been proposed to solve the ambiguity integers [9, 22]. The coordinates of the user receiver are then solved using least squares method.

III. The Effect of Clock Asynchronization of User and Reference Receivers

The receiver records the advance (or recession) of carrier phase during an epoch period, once the signal is locked. A fractional phase measurement is extracted from the carrier loop at the end of each epoch, and the final carrier phase measurement is generated as follows:

$$\phi(t) = \phi(t-1) + \int_{t-1}^{t} f_d(t)\,\mathrm{d}t + \phi_{frac}(t) \tag{8}$$

where:

t , t-1: the current and immediately past epochs

f_d : the Doppler frequency as a function of time

ϕ_{frac} : the measured fractional phase

For an asynchronous PL system, the term f_d in Equation (8) consists of two parts, the motion-induced Doppler frequency $f_{d,motion}$, and the frequency deviation of PL signals $f_{d,pseudolite}$:

$$f_d = f_{d,motion} + f_{d,pseudolite} \tag{9}$$

Substitute Equation (9) into (8), for the PL system as shown in Figure 1, the following relationships exists:

$$\phi_u^i(t) = \phi_u^i(t-1) + \int_{t-1}^{t} f_{d,motion,u}^i(t)\,\mathrm{d}t + \phi_{frac,u}^i(t) + \int_{t-1}^{t} f_{d,pseudolite}^i(t)\,\mathrm{d}t \tag{10}$$

$$\phi_u^j(t) = \phi_u^j(t-1) + \int_{t-1}^{t} f_{d,motion,u}^j(t)\,\mathrm{d}t + \phi_{frac,u}^j(t) + \int_{t-1}^{t} f_{d,pseudolite}^j(t)\,\mathrm{d}t \tag{11}$$

$$\phi_r^i(t) = \phi_r^i(t-1) + \int_{t-1}^{t} f_{d,motion,r}^i(t)\,\mathrm{d}t + \phi_{frac,r}^i(t) + \int_{t-1}^{t} f_{d,pseudolite}^i(t)\,\mathrm{d}t \tag{12}$$

$$\phi_r^j(t) = \phi_r^j(t-1) + \int_{t-1}^{t} f_{d,motion,r}^j(t)\,\mathrm{d}t + \phi_{frac,r}^j(t) + \int_{t-1}^{t} f_{d,pseudolite}^j(t)\,\mathrm{d}t \tag{13}$$

The single and double differences are:

$$\begin{aligned} {}^u\nabla^r\phi^i = {} & \phi_u^i(t-1) + \int_{t-1}^{t} f_{d,motion,u}^i(t)\,\mathrm{d}t + \phi_{frac,u}^i(t) \\ & + \int_{t-1}^{t} f_{d,pseudolite}^i(t)\,\mathrm{d}t - \phi_r^i(t-1) - \int_{t-1}^{t} f_{d,motion,r}^i(t)\,\mathrm{d}t \\ & - \phi_{frac,r}^i(t) - \int_{t-1}^{t} f_{d,pseudolite}^i(t)\,\mathrm{d}t \end{aligned} \tag{14}$$

$$\begin{aligned} {}^u\nabla^r\phi^j = {} & \phi_u^j(t-1) + \int_{t-1}^{t} f_{d,motion,u}^j(t)\,\mathrm{d}t + \phi_{frac,u}^j(t) \\ & + \int_{t-1}^{t} f_{d,pseudolite}^j(t)\,\mathrm{d}t - \phi_r^j(t-1) - \int_{t-1}^{t} f_{d,motion,r}^j(t)\,\mathrm{d}t \\ & - \phi_{frac,r}^j(t) - \int_{t-1}^{t} f_{d,pseudolite}^j(t)\,\mathrm{d}t \end{aligned} \tag{15}$$

$${}^i\nabla^j{}_u\Delta_r\phi = {}^u\nabla^r\phi^i - {}^u\nabla^r\phi^j \tag{16}$$

In a typical receiver, an internal signal with a programmable period, called TIC, is generated to latch measurement data (e.g. carrier phase measurements). An epoch is derived from TIC. Assume that one epoch interval is equal to the TIC period, which can be calculated as:

$$t_{epoch}^u = T_u = P\frac{1}{f_c + \Delta f_u} \tag{17}$$

$$t_{epoch}^r = T_r = P\frac{1}{f_c + \Delta f_r} \tag{18}$$

where:

t_{epoch}^u, t_{epoch}^r: one epoch interval in user and reference receivers, respectively

T_u, T_r: TIC period

P: preset value of the TIC counter (a down counter)

f_c: master clock of the receiver

Δf_u, Δf_r: frequency deviations of user and reference oscillators at the master clock frequency

The difference between one epoch interval of user and reference receivers is:

$$\begin{aligned} \Delta t &= t_{epoch}^u - t_{epoch}^r \\ &= P\left(\frac{1}{f_c + \Delta f_u} - \frac{1}{f_c + \Delta f_r}\right) \end{aligned} \tag{19}$$

Taking this fact into consideration, the terms $\left(\int_{t-1}^{t} f_{d,pseudolite}^i(t)\,\mathrm{d}t - \int_{t-1}^{t} f_{d,pseudolite}^i(t)\,\mathrm{d}t\right)$ and $\left(\int_{t-1}^{t} f_{d,pseudolite}^j(t)\,\mathrm{d}t - \int_{t-1}^{t} f_{d,pseudolite}^j(t)\,\mathrm{d}t\right)$ in Equations (14) and (15) are rephrased as follows:

$$\begin{aligned} \int_{t-1}^{t} f_{d,pseudolite}^i(t)\,\mathrm{d}t - \int_{t-1}^{t} f_{d,pseudolite}^i(t)\,\mathrm{d}t = {} & t_{epoch}^u f_{d,pseudolite}^i(t) \\ & - t_{epoch}^r f_{d,pseudolite}^i(t) \end{aligned} \tag{20}$$

$$\begin{aligned} \int_{t-1}^{t} f_{d,pseudolite}^j(t)\,\mathrm{d}t - \int_{t-1}^{t} f_{d,pseudolite}^j(t)\,\mathrm{d}t = {} & t_{epoch}^u f_{d,pseudolite}^j(t) \\ & - t_{epoch}^r f_{d,pseudolite}^j(t) \end{aligned} \tag{21}$$

Subtracting Equations (20) and (21), the residual error, $\varepsilon^{i,j}$, in the double difference of carrier phase measurements, ${}^i\nabla^j{}_u\Delta_r\phi$, is:

$$\begin{aligned} \varepsilon^{i,j} &= \left(t_{epoch}^u f_{d,pseudolite}^i(t) - t_{epoch}^r f_{d,pseudolite}^i(t)\right) \\ &\quad - \left(t_{epoch}^u f_{d,pseudolite}^j(t) - t_{epoch}^r f_{d,pseudolite}^j(t)\right) \\ &= \left(t_{epoch}^u - t_{epoch}^r\right)\left(f_{d,pseudolite}^i(t) - f_{d,pseudolite}^j(t)\right) \\ &= \Delta t \cdot \Delta f(t) \end{aligned} \tag{22}$$

where $\Delta f(t) = f_{d,pseudolite}^i(t) - f_{d,pseudolite}^j(t)$ is the frequency deviation between the *i*th and *j*th PL

It is clear that the carrier phase measurement error caused by the frequency deviation between PLs cannot be thoroughly removed. The residual error would finally affect the positioning result.

IV. Experiments and Analysis

A. Test set up

Since this paper forces on the investigation of the effect of receiver clock asynchronization and the frequency deviation between PLs, only two PLs are used in the test to implement one-dimension positioning. The test set up is shown in Figure 2. Coordinates of the PLs and the reference receiver are known exactly. The user receiver is located on the origin of coordinates, and it keeps static during the test. The user coordinate X is to be fixed, while Y is fixed to zero.

The carrier frequency of the PL is 1575.42MHz, and the nominal frequency of their frequency sources (OCXO) are both 10MHz. In general, the stability of a reference oscillator should be at least two or three orders of magnitude better than the oscillator used in a low-cost receiver [26]. Therefore, the reference in this paper uses an OCXO as its frequency source,

but the user's frequency source is a TCXO with the nominal frequency of 10MHz. The master clock of the receiver is 39 MHz. The intermediate frequency of both receivers is 0.42MHz with a sampling rate of 39MHz. Locations of the two PLs and reference receiver are shown in Table 1.

TABLE I
LOCATIONS OF THE TWO PLS AND REFERENCE RECEIVER

Item	Coordinate (m)
PL1	(0, -1.780)
PL2	(-0.795, -1.780)
Reference receiver	(-0.452, -0.777)

Two series of tests are conducted to investigate the impact of frequency deviations between PLs and the clock asynchronization of receivers, respectively. The experiment time for each test operation is set for about 6 minutes.

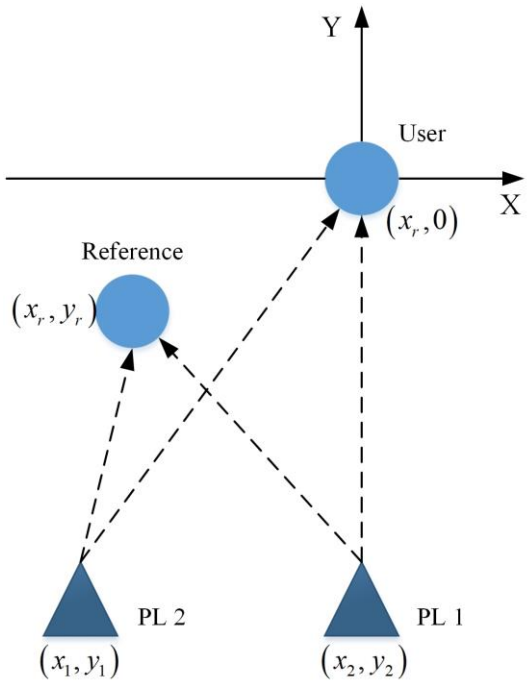

Fig. 2. Test set up of an 1D asynchronous pseudolite navigation system

B. Series 1:

The purpose of this series of tests is to investigate the effect of the frequency deviation between PLs on the carrier phase measurements and the positioning results. The configurations of the interval of one epoch, t_{epoch} and the frequency deviation between the two PLs, Δf , are listed in Table 2. The frequency deviation control is implemented by adjusting the input voltage of the OCXO, which is described in subsection IV.D.

TABLE II
CONFIGURATIONS OF THE INPUT PARAMETERS

Item	Value	Unit
t_{epoch}	0.3	s
Δf	120 500	Hz

1) $\Delta f = 120$Hz

The frequency deviation is planned to be adjusted to about 120Hz. Double difference of carrier phase measurements is shown in Figure 5(a). The mean value of $\varepsilon^{i,j}$ is 2.1497e-4 cycles. The real frequency deviation is 121.2Hz (estimated by differencing the carrier frequency extracted from the two carrier loops in either of the user and reference receiver). According to Equation (22), $\Delta t = \varepsilon^{i,j} / \Delta f = 1.7737\text{e}-6$ s. According to Equation (19), a direct way of estimating Δt is measuring the frequency deviations from nominal frequency of reference oscillators using a frequency counter or spectrum analyzer. The measured frequency deviations are $\Delta f_u = 264.4$Hz and $\Delta f_r = 264.4$Hz at 39MHz. As the nominal interval of one epoch (here is equal to the TIC period) is 0.3s, P is set to $(0.3 \times 39\text{e}6 - 1)$. Substituting these parameters into Equation (19), Δt is found to be -1.7023e-6 s for TIC period of 0.3s, which agrees with experimental results. The theoretical residual error in double difference of carrier phase is 2.0632e-4 cycles for $\Delta f = 121.2$ Hz. The experimental result is shown in Figure 3(a), which is in accordance with the theoretical value, considering the measurement error.

Note that, the impact on the final position is accumulative, according to Equation (8). The result of coordinate X diverges with time as shown in Figure 3(b).

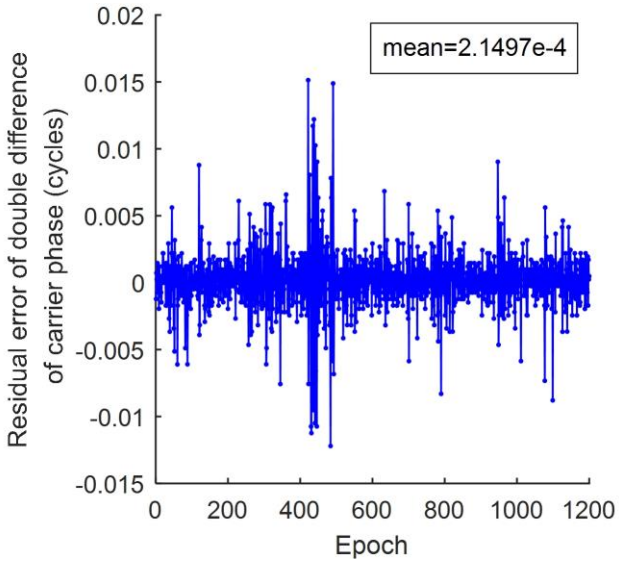

(a)

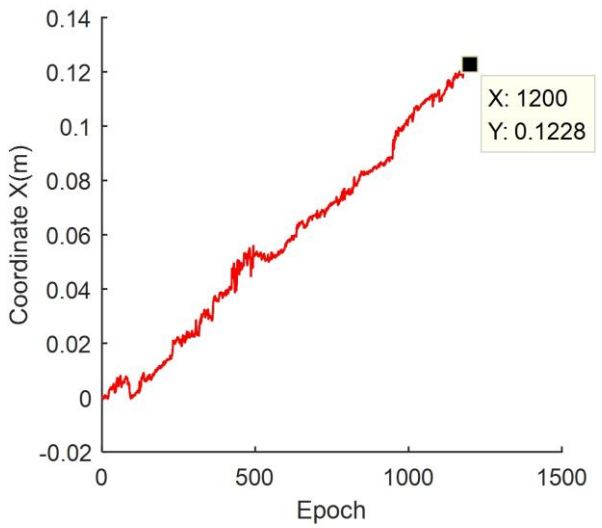

(b)

Fig. 3. $\Delta f \approx 120$ Hz and $t_{epoch} = 0.3$ s: (a) Residual error of double difference of carrier phase advance in one epoch interval; (b) Coordinate X of the user receiver.

2) $\Delta f = 500$Hz

In this test, the frequency deviation between PLs is now increased to about 500Hz. As expected, the residual error of double difference of carrier phase measurements would increases proportionally, as shown in Figure 4(a). The mean value is about 4.12 (8.8524e-4/2.1497e-4) times of that when Δf is about 120Hz. The actual frequency deviation in this test is 502.9Hz, namely about 4.15 (502.9/121.2) times larger. The results demonstrate the reasonability of Equation (22). The positioning result is shown in Figure 4(b). At epoch #1200, the coordinate X is 0.5606 m, which is about 4.57 (0.5606/0.1228) times bigger than that in Figure 3(b).

As a conclusion, this series of tests indicate that, the frequency deviation between PLs cannot be thoroughly wiped off via double difference method, due to the asynchronous clocks between receivers. The residual error is proportional to this frequency deviation.

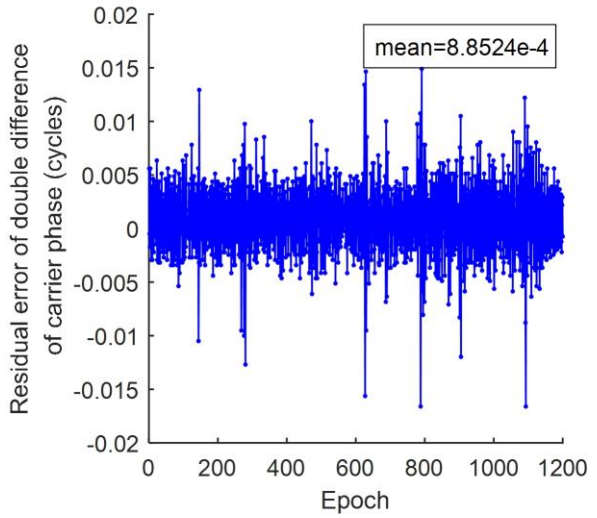

(a)

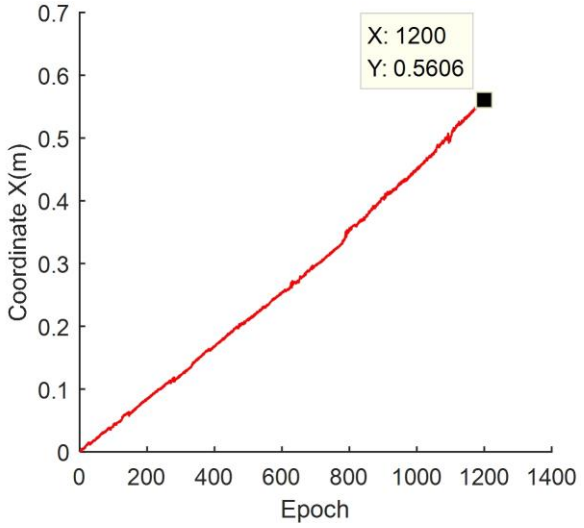

(b)

Fig. 4. $\Delta f \approx 500$ Hz and $t_{epoch} = 0.3$ s: (a) Residual error of double difference of carrier phase advance in one epoch interval; (b) Coordinate X of the user receiver.

C. Series 2:

In this series of tests, the fixed frequency deviation between PLs, Δf and the different interval of one epoch, t_{epoch} are set to evaluate the impact on the residual error of double difference of carrier phase and the positioning performance. The detailed parameters configurations are listed in Table 3.

TABLE III
CONFIGURATIONS OF THE INPUT PARAMETERS

Item	Value	Unit
t_{epoch}	0.6 1	s
Δf	120	Hz

By changing the value of P, the TIC period can be adjusted. Again, assume that one epoch interval is identical to the TIC period. The results are shown in Figures 5 and 6 for $t_{epoch} = 0.6$ s and 1.0 s, respectively. Table 4 shows the experimental and theoretical values of residual errors for different epoch interval. The experimental results are in good agreement with the theoretical ones. This series of tests indicate that the residual error due to frequency deviation between PLs is also proportional to the observation time

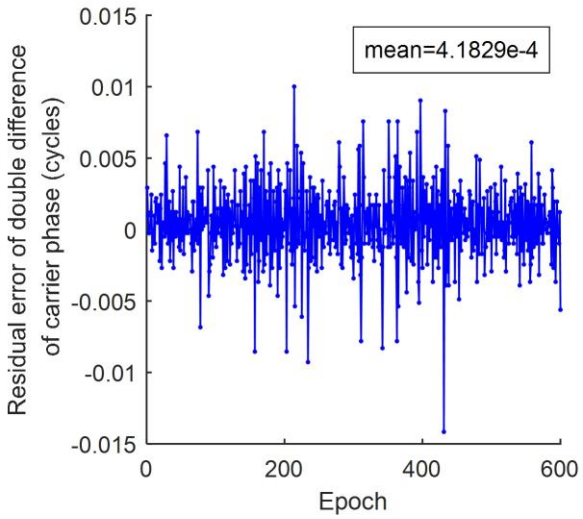

Fig. 5. $\Delta f \approx 120$ Hz and $t_{epoch} = 0.6$ s: (a) Residual error of double difference of carrier phase advance in one epoch interval; (b) Coordinate X of the user receiver.

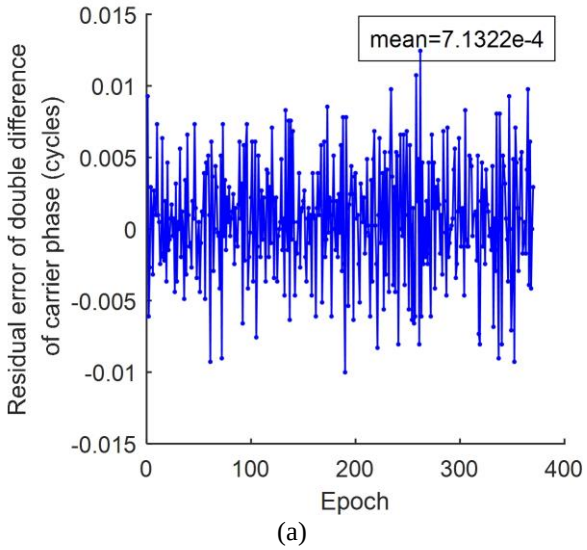

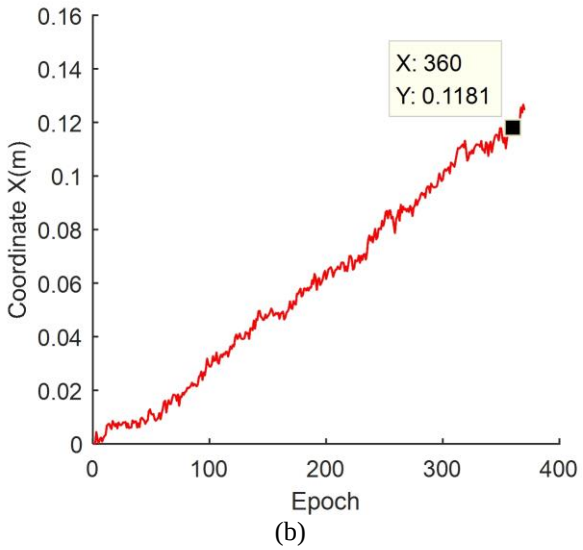

Fig. 6. $\Delta f \approx 120$ Hz and $t_{epoch} = 1$ s: (a) Residual error of double difference of carrier phase advance in one epoch interval; (b) Coordinate X of the user receiver.

TABLE IV
RESULTS OF RESIDUAL ERRORS OF DOUBLE DIFFERENCE MEASUREMENTS FOR DIFFERENT EPOCH INTERVAL

t_{epoch} (s)	$\varepsilon^{i,j}$ (cycle)		
	Experimental value	Theoretical value	Percentage error
0.3	2.1497e-4	2.0632e-4	4.19%
0.6	4.1829e-4	4.1264e-4	1.37%
1.0	7.1322e-4	6.8773e-4	3.71%

D. Solutions to this problem

According to Equation (22) and the above experimental results, the carrier phase measurement error caused by frequency deviation between PLs is determined by the term Δt and Δf . Therefore, the residual error can be reduced by decreasing either of these two terms. Both of them are determined by the frequency source, refer to the OCXO used in PLs navigation system. Fortunately, the output frequency of the OCXO can be adjusted by controlling its input voltage. For the asynchronous PL system, one solution is to synchronize the carrier frequency of PLs, or to synchronize the clock of receivers by changing the output frequency of their frequency sources, based on the estimated Δt and Δf .In this paper, the latter is objective. To achieve this, we propose two methods. One is refer to hardware method The other one, which is referred as software method here, is to correct the residual error in the carrier phase double difference in the navigation solver.

1) *Hardware method*

In subsection IV.B and IV.C, the control of frequency deviation between PLs is implemented by hardware method, where the input voltage of the OCXO of the PL is adjusted. Specifically, the adjustment was first obtained based on the estimated frequency deviation in the user receiver by differencing the carrier frequency of the two carrier loops. The adjustment information was then sent to the PL via a wireless data link. Finally, the MCU unit adjusts the OCXO input

voltage of the PL according to the information provided by the wireless serial port module, to eliminate the frequency deviation. Figure 7 shows the OCXO control module of PL.

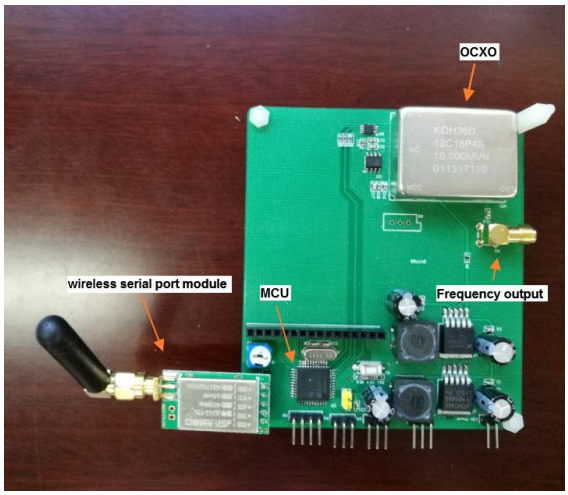

Fig. 7. The OCXO control module

To reduce the residual error in double difference of carrier phase, the frequency deviation is desired to be reduced to 0 Hz. Figure 8 shows the final frequency deviation between the two PLs, where the mean value is about -0.4678Hz. Considering Equation (22), the residual error, $\varepsilon^{i,j}$, caused by frequency deviation between PLs is negligible during a test of 6 minutes. Figure 9(a) shows the double difference of carrier phase advance in the interval of one epoch between two receivers. The mean value of the residual error is 5.7592e-6 cycles, which is close to the desired value, 0 cycles. The coordinate X of the user receiver is shown in Figure 9(b), where the maximum deviation does not exceed 7 mm during about 6 minutes.

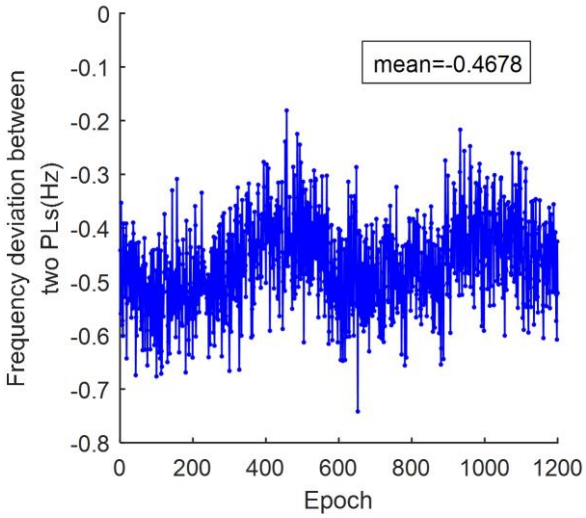

Fig. 8. Frequency deviation between two PLs extracted from the user receiver

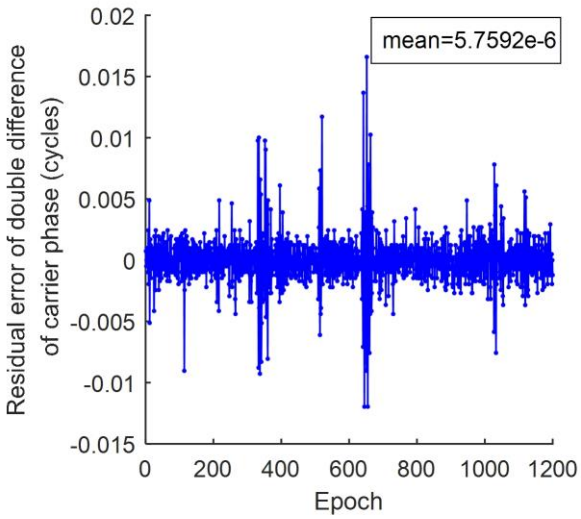

(a)

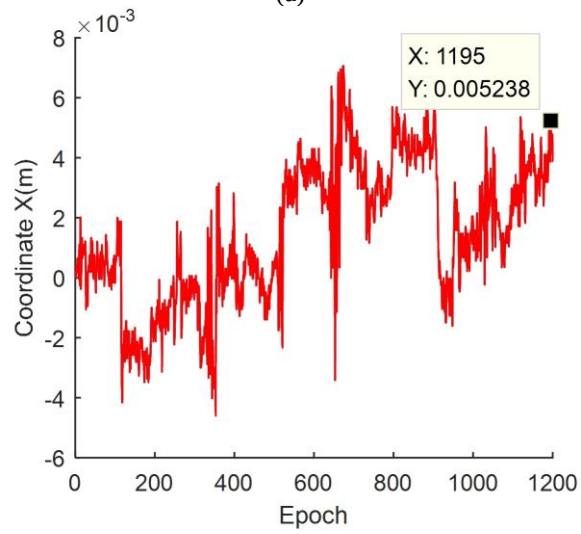

(b)

Fig. 9. $\Delta f \approx 0$ Hz and $t_{epoch} = 0.3$ s: (a) residual error of double difference of carrier phase advance in one epoch interval; (b) coordinate X of the user receiver.

2) *Software method*

Inspired by the tests above, the residual error in double difference of carrier phase can be estimated after an initialization period (e.g. 400 epochs) since these phase residuals are tend to be around zero. Specifically, the measured phase residuals of the PL signal are first obtained by the reference receiver. The reference then provides data compensation with these measurements. Finally, the carrier phase measurements could be corrected using this compensation information. Figure 10 shows the coordinate X of the user using this method, where $\Delta f \approx 120$ Hz and $t_{epoch} = 0.3$ s. The coordinate X of the user diverges during the first 400 epochs, and is corrected after 400 epochs using the estimated residual error.

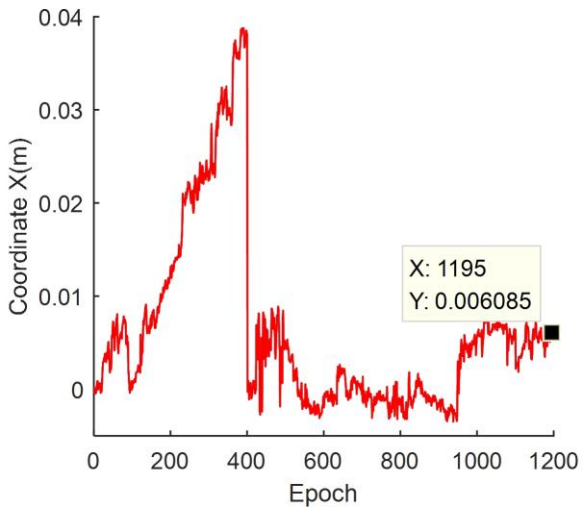

Fig. 10. Coordinate X of the user

V. Conclusions

In this paper, the effect of frequency deviation between PLs and time deviation between user and reference receivers are considered in an asynchronous PL navigation system. Carrier phase double differences positioning algorithm is at first derived. Considering the fact that there exists time deviation due to the asynchronous clocks of user and reference receivers, the frequency deviation between PL signals cannot be thoroughly removed via the double difference method. The residual error in the double difference of carrier phase measurements are deduced, which is found to be proportional to the frequency deviation between PLs and the time deviation between receivers. Two series of experiments are conducted to verify the proposed idea from the perspective of frequency deviation between PLs, and time division between receiver clocks, respectively. Moreover, two approaches to solve this problem are proposed. The experimental results prove the feasibility and effectiveness of the methods.

In our future work, we will evaluate the performance of the methods in high-dynamic PLs applications.

References

[1] L. T. Hsu, Y. Gu, Y. Huang, and S. Kamijo, "Urban Pedestrian Navigation Using Smartphone-Based Dead Reckoning and 3-D Map-Aided GNSS," IEEE Sens. J., vol. 16, no. 5, pp. 1281–1293, 2016, doi: 10.1109/JSEN.2015.2496621.

[2] A. S. El-wakeel, S. Member, A. Osman, N. Zorba, and S. Member, "Robust Positioning for Road Information Services in Challenging Environments," IEEE Sens. J., vol. 20, no. 6, pp. 3182-3195, 15 March15, 2020, doi: 10.1109/JSEN.2019.2958791.

[3] B. Xu, Q. Jia, and L.-T. Hsu, "Vector Tracking Loop-Based GNSS NLOS Detection and Correction: Algorithm Design and Performance Analysis," IEEE Trans. Instrum. Meas., 2019, doi: 10.1109/tim.2019.2950578.

[4] Elrod, B.D. and Van Dierendonck, A.J. (1996), Pseudolites in Global Positioning System, Theory and Applications. American Institute of Aeronautics and Astronautics (AIAA), 2(2), 51–79.

[5] Kee, C.; Jun, H.; Yun, D.; Kim, B.; Kim, Y.; Parkinson, B.W.; Langenstein, T.; Pullen, S.; Lee, J. Development of Indoor Navigation System Using Asynchronous Pseudolites. In Proceedings of the 13th International Technical Meeting of the Satellite Division of The Institute of Navigation (ION GPS 2000), Salt Lake City, UT, USA, 19–22 September 2000; pp. 1038–1045.

[6] Barnes J, Rizos C, Kanli M, Small D, Voigt G, Gambale N, Lamance J, Nunan T, Reid C (2004) Indoor industrial machine guidance using Locata: a pilot study at BlueScope Steel. In: 60th annual meeting of the US Institute of Navigation, Dayton, Ohio, 7–9 June, pp 533–540.

[7] C. Kim, H. So, T. Lee, and C. Kee, "A Pseudolite-Based Positioning System for Legacy GNSS Receivers," pp. 6104–6123, 2014, doi: 10.3390/s140406104.

[8] C. Sheng, X. Gan, B. Yu, and J. Zhang, "Precise point positioning algorithm for pseudolite combined with GNSS in a constrained observation environment," Sensors (Switzerland), vol. 20, no. 4, 2020, doi: 10.3390/s20041120.

[9] X. Wan, C. Zhai, and X. Zhan, "The pseudolite-based indoor navigation system using ambiguity resolution on the fly," ISSCAA2010 - 3rd Int. Symp. Syst. Control Aeronaut. Astronaut., pp. 212–217, 2010, doi: 10.1109/ISSCAA.2010.5633076.

[10] C. Rizos, G. Roberts, J. Barnes, and N. Gambale, "Experimental results of Locata: A high accuracy indoor positioning system," 2010 Int. Conf. Indoor Position. Indoor Navig. IPIN 2010 - Conf. Proc., no. September, pp. 15–17, 2010, doi: 10.1109/IPIN.2010.5647717.

[11] W. Jiang, Y. Li, and C. Rizos, "Locata-based precise point positioning for kinematic maritime applications," GPS Solut., vol. 19, no. 1, pp. 117–128, 2014, doi: 10.1007/s10291-014-0373-9.

[12] A. V. Picois and N. Samama, "Near-far interference mitigation for pseudolites using double transmission," IEEE Trans. Aerosp. Electron. Syst., vol. 50, no. 4, pp. 2929–2941, 2014, doi: 10.1109/TAES.2014.090292.

[13] C. O'Driscoll, D. Borio, and J. Fortuny-Guasch, "Investigation of pulsing schemes for pseudolite applications," 24th Int. Tech. Meet. Satell. Div. Inst. Navig. 2011, ION GNSS 2011, vol. 5, no. April, pp. 3480–3492, 2011.

[14] D. Borio and C. O'Driscoll, "Design of a general pseudolite pulsing scheme," IEEE Trans. Aerosp. Electron. Syst., vol. 50, no. 1, pp. 2–16, 2014, doi: 10.1109/TAES.2013.110277.

[15] J. Barnes, C. Rizos, M. Kanli, and A. Pahwa, "A positioning technology for classically difficult GNSS environments from Locata," Rec. - IEEE PLANS, Position Locat. Navig. Symp., vol. 2006, pp. 715–721, 2006, doi: 10.1109/PLANS.2006.1650665.

[16] L. Dai, "Augmentation of GPS with GLONASS and pseudolite signals for carrier phase-based kinematic positioning", PhD thesis, 2002, the University of New South Wales.

[17] Söderholm, S.; Jokitalo, T. "Synchronized Pseudolites - The Key to Indoor Navigation," *Proceedings of the 15th International Technical Meeting of the Satellite Division of The Institute of Navigation (ION GPS 2002)*, Portland, OR, September 2002, pp. 226-230.

[18] J. E. Lee and S. Lee, "Indoor initial positioning using single clock pseudolite *system*," 2010 Int. Conf. Inf. Commun. Technol. Converg. ICTC 2010, pp. 575–578, 2010, doi: 10.1109/ICTC.2010.5674761.

[19] D. Borio, C. Gioia, and G. Baldini, "Asynchronous pseudolite navigation using C/N0 *measurements*," J. Navig., vol. 69, no. 3, pp. 639–658, 2016, doi: 10.1017/S037346331500082X.

[20] J. Barnes, C. Rizos, and J. Wang, "Locata : the positioning technology of the future ?," *6th Int. Symp. Present. SatNav 2003 Satell. Navig. Technol. Incl. Mob. Position. Locat. Serv.*, vol. 49, no. January, pp. 1–14, 2003.

[21] J. Barnes, C. Rizos, and J. Wang, "Locata : the positioning technology of the future ?," *6th Int. Symp. Present. SatNav 2003 Satell. Navig. Technol. Incl. Mob. Position. Locat. Serv.*, vol. 49, no. January, pp. 1–14, 2003.

[22] X. Guo, Y. Zhou, J. Wang, K. Liu, and C. Liu, "Precise point positioning for ground-based navigation systems without accurate time synchronization," *GPS Solut.*, vol. 22, no. 2, 2018, doi: 10.1007/s10291-018-0697-y.

[23] H. So et al., "Implementation of a vector-based tracking loop receiver in a pseudolite navigation system," Sensors, vol. 10, no. 7, pp. 6324–6346, 2010, doi: 10.3390/*s100706324*.

[24] B. Xu and L. Dou, "GNSS IF Signal Simulation Considering Oscillator Phase Noise," J. Navig., vol. 70, no. 4, pp. 805–820, 2018, doi: 10.1017/s0373463318000036.

Jie Dou received the B. S. degree in communication engineering from Hunan University of Technology in 2013. He is currently pursuing the Ph.D. degree in navigation guidance and control from Nanjing University of Science and Technology, China. His research interests are related to GNSS and pseudosatellite positioning system.

Bing Xu is currently an assistant professor with Interdisciplinary Division of Aeronautical and Aviation Engineering, The Hong Kong Polytechnic University. He received his B.S. and PhD. degrees in network engineering and navigation guidance and control from Nanjing University of Science and Technology, China, in 2012 and 2018, respectively. His research focuses on signal processing, wireless communications, Global Navigation Satellite Systems, machine learning.

Lei Dou was born in Lianyungang, China, in 1974. He received the B.Eng. degree in chemical engineering, M.Eng. degree in power engineering and Ph.D. degree in automation from Nanjing University of Science and Technology, Nanjing, China, in 1996, 2003 and 2006, respectively.

Since 2009, he has been an associate professor with National Key Laboratory of Transient Physics, Nanjing University of Science and Technology. His current research interests include guidance and control, artificial intelligence.